한국광물학회지 제 17 권 제 1 호 (2004년 3월)
J. Miner. Soc. Korea, 17(1), 11-21 (March, 2004)

Precipitation of $CaCO_3$ Crystals from Variously Supersaturated Solutions

다양한 과포화 조건하에서의 탄산염광물의 합성에 대한 연구

Hyeon Yoon (윤 혜 온)[1,*] and Soo Jin Kim (김 수 진)[2]

[1]Korea Basic Science Institute, Hazardous Substances Research Team, Seoul 136-701, Korea
(한국기초과학지원연구원 유해물질분석연구팀)
[2]School of Earth and Environmental Science, Seoul National University, Seoul 151-742, Korea
(서울대학교 지구환경과학부)

ABSTRACT : Crystallization of $CaCO_3$ from the solutions of various degrees of supersaturation was carried out by a spontaneous precipitation method. The solution was kept at 25℃ and pH 6.9~8.8. The solution compositions were varied in two ways: (1) The total carbonate, $[CO_3]_T$ to total calcium, $[Ca]_T$, ratios vary as ; $[CO_3]_T/[Ca]_T > 1$, $[CO_3]_T/[Ca]_T = 1$, and $[CO_3]_T/[Ca]_T < 1$. (2) The total calcium concentration, $[Ca]_T$, held at 0.02 mol/dm^3, 0.2 mol/dm^3, and 0.4 mol/dm^3.

We found that the $CaCO_3$ phase crystallized from the solutions of $[CO_3]_T/[Ca]_T \geq 1$ was mostly calcite with less than 1% of vaterite, while the $CaCO_3$ crystals precipitated from low carbonate concentration toward calcium concentration, $[CO_3]_T/[Ca]_T < 1$, were dominated by vaterite crystals. It appears that the polymorph of $CaCO_3$ precipitate was mainly controlled not by the calcium concentration but by the carbonate concentration during the spontaneous precipitation. Also, we found that the surface roughness of vaterite increased with decreasing carbonate concentration from 0.8 or 0.5 of $[CO_3]_T/[Ca]_T$ ratios and the surface area of vaterite increased from 5.64~7.34 μm to 8.39~10.3 μm.

Key words : $CaCO_3$ crystallization, spontaneous precipitation method, $[CO_3]_T/[Ca]_T$ ratio, calcite, vaterite

요약 : 자발적 침전법에 의하여 다양한 과포화 용액에서 탄산염광물을 합성하였다. 합성용액의 온도는 25℃에서 유지 시켰고 pH범위는 6.9에서 8.8 이였다. 용액의 과포화도 조절 시 2가지 변수를 두어 농도를 변화 시켰다. (1) total carbonate의 농도와 total calcium의 농도비가 다음 세가지 조건을 만족시키도록 변화시켰다: $[CO_3]_T/[Ca]_T > 1$, $[CO_3]_T/[Ca]_T = 1$, and $[CO_3]_T/[Ca]_T < 1$. (2) 앞서 언급한 조건에 total calcium의 농도를 0.02 mol/dm^3, 0.2 mol/dm^3, 그리고 0.4 mol/dm^{3}이 되도록 변화 시켰다.

$[CO_3]_T/[Ca]_T \geq 1$의 조건하에서 형성된 미립의 탄산염 광물은 대부분 거의 순수한 방해석으로 바테라이트가 1% 이하로 존재하였으며 이와는 달리 $[CO_3]_T/[Ca]_T < 1$ 조건하에서는 거의 순수한 바테라이트가 합성되었다. 본 연구 결과 탄산염광물의 상은 합성 용액상의 $[CO_3]_T$농도 보다는 $[CO_3]_T$의

*Corresponding Author (교신저자): dunee@kbsi.re.kr

농도에 의하여 좌우되는 것으로 나타났다. 또한 바테라이트의 합성 결과는 $[CO_3]_T/[Ca]_T$의 비가 0.8에서 0.5로 낮아짐에 따라 roughness가 증가하고 결과적으로 광물표면적이 5.64~7.34 μm에서 8.39~10.3 μm로 증가한다.

주요어 : 탄산염 광물 합성, 자발적 침전법, $[CO_3]_T/[Ca]_T$ 성분비, 방해석, 바테라이트

Introduction

Calcium carbonate, $CaCO_3$, is one of the most abundant phases in natural environment. It contains various sorbed species on the surface and coprecipitates in the crystal, including heavy metals which reflect the mineral formation environment and alteration history (Zhong and Mucci, 1995). Calcium carbonate is also important in many fields such as geochemical cycles of CO_2 and removal of metal ions from effluent streams. The precipitation of calcium carbonate minerals has become an important concern in industrial boilers, transportation pipes, even in the desalination plants where the concentration of calcium and carbonate exceeds the saturation level (de Leeuw and Parker, 1998). Many researchers also have noticed the strong interactions between surface of calcium carbonates and heavy metals from various natural environments (Davis *et al.*, 1987; Zachara *et al.*, 1991).

Because a simple but effective way of removing metal ions from wastewater is using mineralwater interfacial reactions, characterization of mineral surfaces becomes important. One of the principal goals of characterizing solid surfaces is to establish a correlation between the mechanisms of their formation and their physical and chemical properties during their interactions with dissolved species.

Calcium carbonate minerals formed from various natural environments exhibit characteristic surface morphologies depending on their growth solution conditions and secondary alteration histories. Highly supersaturated solutions often produce minerals of more complicated surface morphology while minerals from diluted solutions precipitate of simple surface morphology (Mullin, 1991).

Surface-sensitive microscopic and spectroscopic techniques illustrate that chemical reactivity of solid surface plays a crucial role in dissolution and sorption reactions (Liang and Baer, 1997). The surface structure of calcium carbonate minerals has been studied by a variety of methods such as AFM and SEM both under ultrahigh vacuum conditions. AFM observations have demonstrated that calcite grows from aqueous solution by motion of monomolecular steps, and dissolves by a combination of step motion and etch pit expansion (Hillner *et al.*, 1992; Dove and Hochellar, 1993). Along this line of study, relationship between growth mechanisms and the shape of calcite crystals and size distributions were tested and observed under Scanning Electron Microprobe (Kile *et al.*, 2000).

Additionally, the equilibrium surface morphology of carbonate polymorphs was predicted based on calculations of surface free energy (Titiloye *et al.*, 1998; de Leeuw and Parker, 1998). The surface cationic sites were compared for the site preference of certain metal ions or certain mineral structures such as calcite or dolomite.

In this study, the differences in surface morphology and surface sites were discussed based on equilibrium surface energies. This study will aid to understand the different surface morphology of $CaCO_3$ and their reactivity for metal ions from various natural environments. The surface morphology, the surface areas, and the size of each $CaCO_3$ precipitates were discussed in relation to each other regarding rendering effective surface site for metal interaction.

Experimental Method

The calcium carbonate, $CaCO_3$, crystals were prepared by a spontaneous precipitation method from solutions of three different ratios of total carbonate, $[CO_3]_T$ over total calcium, $[Ca]_T$,: $[CO_3]_T/$

Table 1. Precipitation systems for different synthetic $CaCO_3$ crystals by spontaneous precipitation method and their physical parameters

System	Type of $CaCO_3$	$[CO_3]_T/[Ca]_T$	$[Ca]_T$ (mol/dm^3)	*mean size (μm)	**surface area (m^2/g)
I	Calcite	1.5	0.02	4.3	1.20
			0.20	7.4	0.64
			0.40	7.5	0.61
		2.0	0.02	3.6	1.50
			0.20	7.0	0.70
			0.40	8.5	0.59
II	Calcites	1.0	0.02	6.1	1.03
			0.20	5.8	1.56
			0.40	7.2	0.92
III	Vaterite	0.5	0.02	10.1	8.39
			0.20	9.1	10.3
			0.40	9.1	10.2
		0.8	0.02	9.5	5.64
			0.20	9.7	5.90
			0.40	10.1	7.34

*Measured by optical measurements and SEM observation.
**Measured by BET method.

$[Ca]_T > 1$, $[CO_3]_T/[Ca]_T = 1$, and $[CO_3]_T/[Ca]_T < 1$. In the first system, the $[CO_3]_T/[Ca]_T$ ratio was adjusted to 1.5 and 2.0. In the third system, the ratio was kept as 0.5 and 0.8 (Table 1). In addition to this fixed $[CO_3]_T/[Ca]_T$ ratio, the total calcium concentration was varied to 0.02 mol/dm^3, 0.2 mol/dm^3, and 0.4 mol/dm^3 and the corresponding carbonate concentration was changed to hold the given ratios (Table 1).

$CaCO_3$ Precipitation

A common method for producing a precipitate is to mix two reactant solutions together as quickly as possible. This process involves the creation of highly supersaturated systems, but the major difficulty is to maintain reasonably uniform conditions throughout the reaction vessel during the whole reaction time (Mullin, 1991). Therefore, the choice of the method of reactant mixing is very important and should avoid any accidental development of heterogeneous zones of excessive supersaturation. In this study, calcite precipitation was initiated by mixing two concentrated solutions of $CaCl_2 \cdot 2H_2O$ and $(NH_4)_2CO_3$ in a 1000 mL glass reaction vessel. The reaction vessel was immersed in a temperature controlled water bath at 25℃ and 1 atm, and continuously stirred by rotating the propeller at 250~300 rpm. The reaction vessel was covered by an acrylic plate but not sealed. Almost instantaneous precipitation of calcium carbonates was observed. The precipitation was usually lasted for a few minutes. When the suspension became cleared after 5 minutes and then the entire suspension was filtered by polycarbonate membrane filter (0.4 μm polycarbonate membrane, Poretics) and dried at 60℃ for two days. In order to avoid surface modification during filtration, the crystal precipitates were thoroughly washed with saturated solutions with respect to $CaCO_3$. No changes in morphology were observed after drying the samples at 60℃. The reagent grade chemicals used in this study were supplied by Merck (Germany). During $CaCO_3$ precipitation, pH of the solution was not adjusted.

Solution Supersaturation

The composition of the experimental solution was controlled by changing $[Ca]_T$ and $[CO_3]_T$. The level of supersaturation (Ω) was defined as:

$$\Omega = Q / K_{SP}$$

where

$$Q = [H^+] / [Ca^+] [HCO_3^-]$$

in which the brackets refer to activities of dissolved ion in solution, the actual ion activity product Q, and K_{sp} is the solubility product of calcium carbonate.

Size Analysis and Surface Area Measurements

Upon completion of the precipitation experiments, solutions and the crystal precipitates were filtered through 0.4 μm polycarbonate membrane filter. The crystals were taken from membrane filter, placed on a glass slide and the crystal size

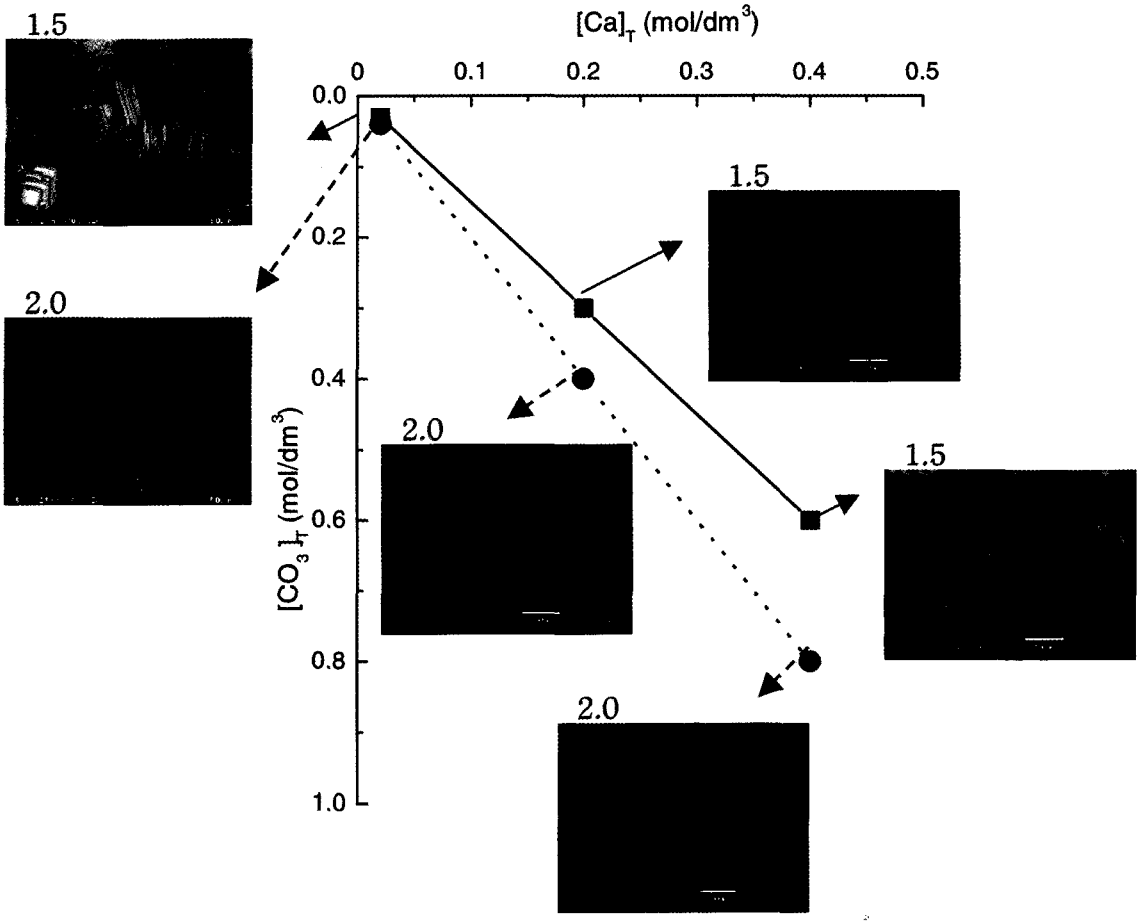

Fig. 1. Synthetic calcite crystals precipitated by instantaneous nucleation method with $[CO_3]_T > [Ca]_T$ molar ratios. 1.5 and 2.0 represent 1.5 and 2.0 molar ratios of $[CO_3]_T$ / $[Ca]_T$.

was measured by microscope (×500). About 250 to 300 individual crystals were measured. Two asymmetric long diagonals were measured of a crystal and averaged as described by Kiel *et al.* (2000). The size of the calcium carbonate precipitates of 50 individual crystals from 5 different sample sections was also measured under SEM (Fig. 1, 2 and 3) (Table 1).

The surface area of calcium carbonate precipitates was determined by the Brunauer-Emmett-Teller (BET) method using Quantachrome Monosorb MS-18. The BET measurement was repeated three times.

Characterization of Calcium Carbonate Precipitates

Phase and purity of the calcium carbonate precipitates were examined by a Philips X-ray diffractometer (X'Pert PW3040) with a continuous scan mode under the conditions of 1°/min scanning speed and 40 kV/30 mA. The morphology of the $CaCO_3$ crystals was observed using a field emission scanning electron microscope (FE-SEM, Hitachi S-4700) with an acceleration voltage of 15 kV.

Results and Discussion

The $CaCO_3$ crystals precipitated from variously supersaturated solutions demonstrated that the

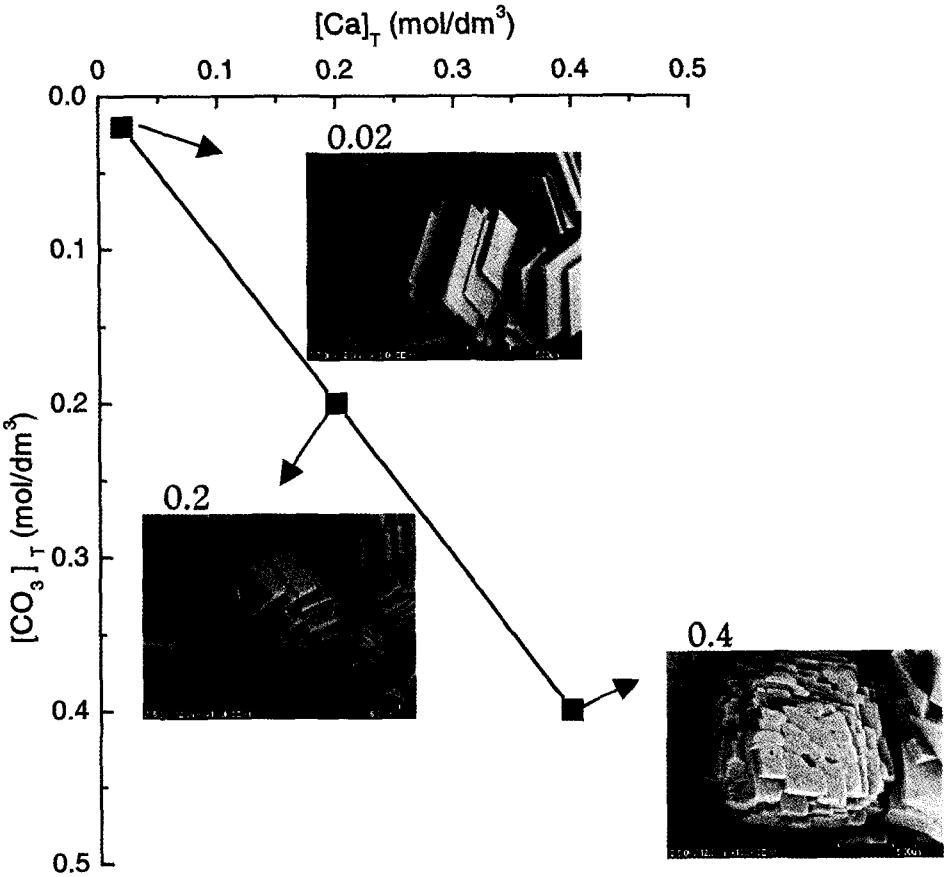

Fig. 2. Synthetic calcite crystals precipitated by instantaneous nucleation method with 1 : 1 of $[CO_3]_T$ / $[Ca]_T$ molar ratio for 0.02 M (a-type), 0.2 M (b-type), and 0.4 M $[Ca]_T$ (c-type), respectively.

surface morphology, the crystal size, and the surface area were related to each other (Fig. 1, 2, and 3). XRD and SEM analyses confirmed that the $CaCO_3$ precipitates prepared under $[CO_3]_T$ / $[Ca]_T \geq 1$ conditions were mostly calcite, while those prepared under $[CO_3]_T$ /$[Ca]_T < 1$ conditions were almost pure vaterite. (Fig. 4). Both vaterite and calcite crystallized during spontaneous precipitation, but in all experiments the amount of vaterite (in the presence of calcite majority) and calcite (in the presence of vaterite majority) were considerably small (less than 1%) compared to that of either calcite or vaterite. The presence of those nearly mutually exclusive $CaCO_3$ polymorphs did not appear to influence the surface morphology even though it would have some effect on the measured surface areas.

$CaCO_3$ Precipitated from the Solutions of $[CO_3]_T / [Ca]_T > 1$

The calcium carbonates precipitated from excess carbonate conditions were mostly calcite crystals of rhombohedral cleavages whereas each calcite crystals exhibited different surface morphologies depending on their solution compositions (Fig. 1).

The total carbonate to calcium ratio was fixed at either 1.5 or 2.0. For each ratio, the calcium concentration was changed to 0.02 mol/dm^3, 0.2 mol/dm^3, and 0.4 mol/dm^3 (Table1). The calcite precipitates were distinguished into two parts depending on total calcium concentration, one

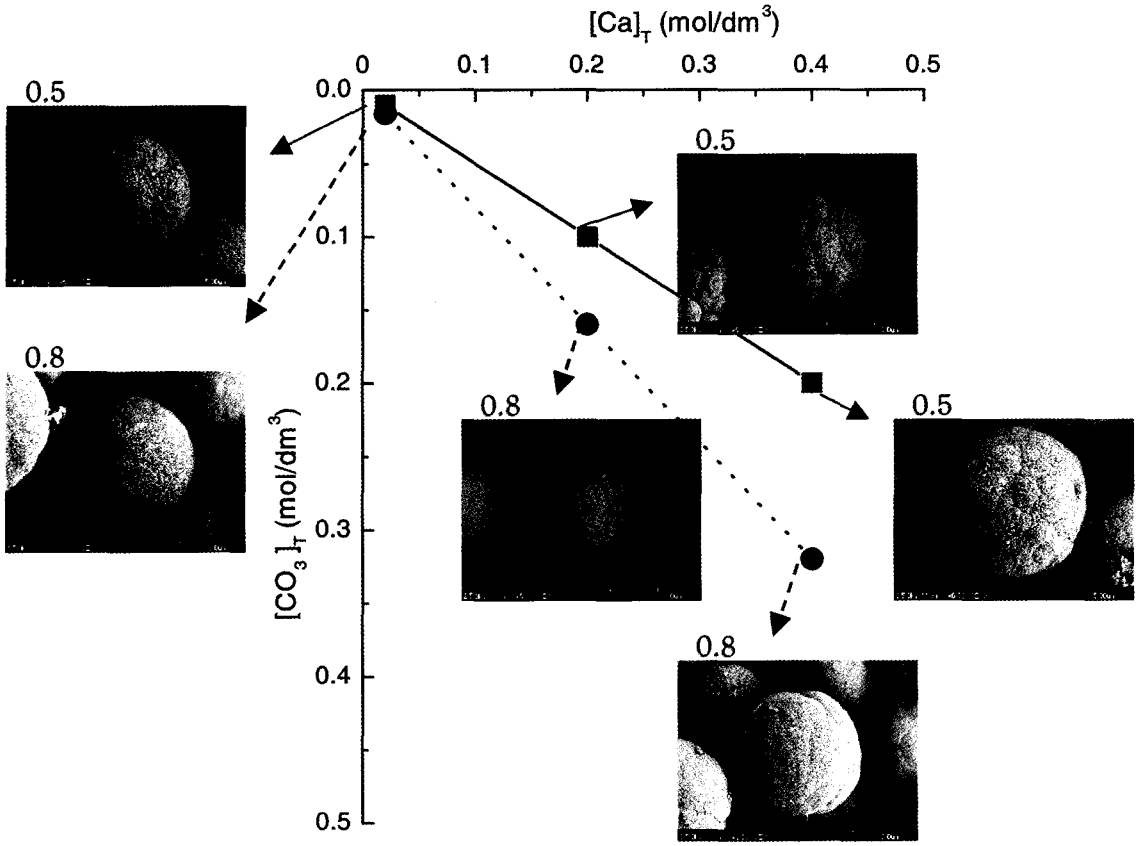

Fig. 3. Synthetic vaterite crystals precipitated by instantaneous nucleation method with $[CO_3]_T < [Ca]_T$ molar ratios. 0.5 and 0.8 represent 0.5 and 0.8 molar ratios of $[CO_3]_T$ / $[Ca]_T$.

from 0.02 mol/dm^3 $[Ca]_T$ solution and the others from both 0.2 mol/dm^3 and 0.4 mol/dm^3 $[Ca]_T$ solutions. With the increase of the total calcium concentration the morphology of the calcite precipitates became less complicated (Fig. 1) but the crystal size became more diversified (Table 1).

The calcite crystals precipitated from 0.02 mol/dm^3 $[Ca]_T$ solution, both 1.5 and 2.0 $[CO_3]_T$ / $[Ca]_T$ ratios exhibited agglomeration of small platelets on one direction parallel to $\{10\bar{1}4\}$. This type of agglomeration becomes more complicated when the total carbonate to total calcium ratio increased to 2.0. The calcite crystals precipitated from these solutions showed almost uniform size, average of 4.3 μm in diameter (Fig. 1).

However, when the calcite was prepareded from the solutions of higher concentrations, 0.2 mol/dm^3 and 0.4 mol/dm^3 $[Ca]_T$, mixed sized crystals were precipitated (Fig. 1). The calcites exhibited less complicated surface morphology compared with the calcite precipitated from 0.02 mol/dm^3 total calcium concentration. The mean size of those calcite crystals is 7.4 μm. SEM observation demonstrated that the calcite exhibit simple cleavage $\{10\bar{1}4\}$ face. There was no evidence of developing agglomeration of small platelets along $\{10\bar{1}4\}$ direction. The occurrence of mixed sized crystals indicates surface textural evolution of the Ostwald ripening; large grains grow at the expense of small crystals (Miyazaki, 1996). This was frequently observed from the solution where over-growth of large crystals continued on behalf of small crystals especially in highly supersaturated solutions. According to Miyazaki (1996), the ripening of large crystals continueuntil the remaining small crystals were

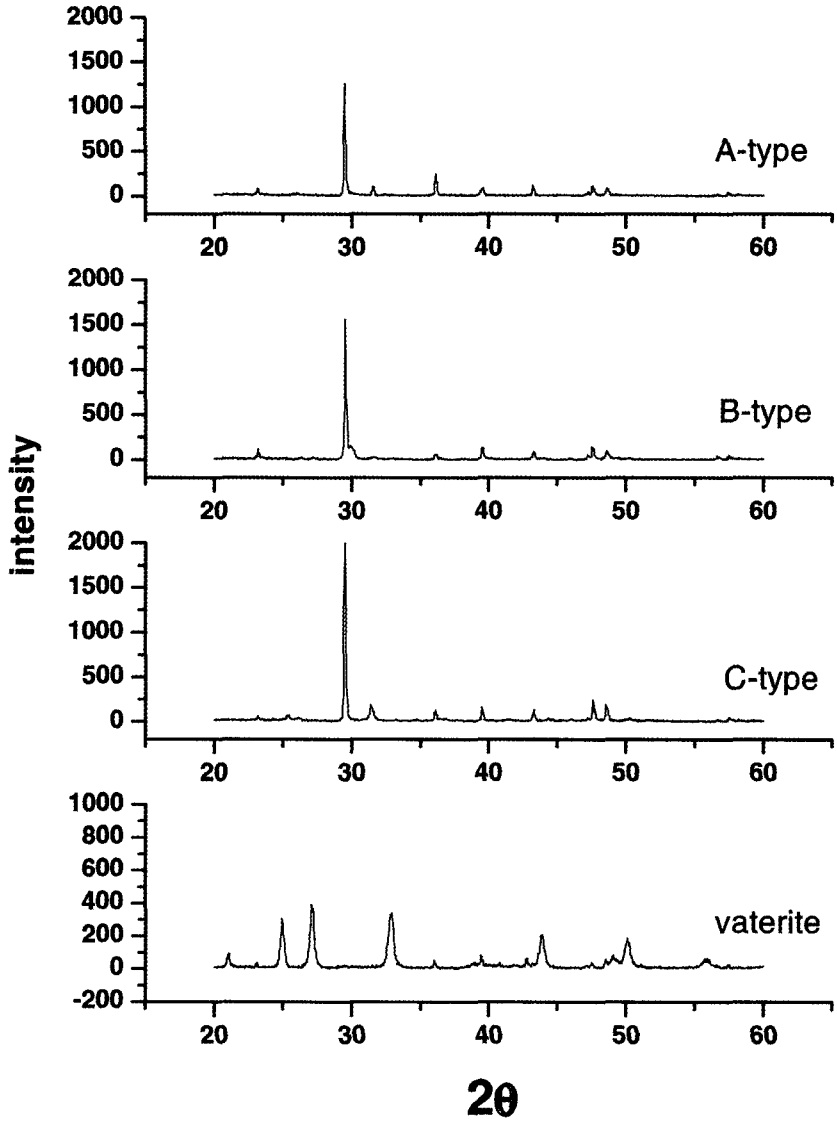

Fig. 4. X-ray powder diffractogram of synthetic calcites and vaterite precipitated from 0.02 M (a-type), 0.2 M (b-type), and 0.4 M $CaCl_2 \cdot 2H_2O$ solution (c-type).

all disappear.

$CaCO_3$ Precipitated from the Solutions of $[CO_3]_T/[Ca]_T = 1$

The calcium carbonate precipitated from the solutions of equal $[CO_3]_T$ to $[Ca]_T$ ratio was almost pure calcite with less than 1% of vaterite. The surfaces of calcite prepared from 0.02 mol/dm^3 and 0.2 mol/dm^3 $[Ca]_T$ were all dominated by $\{10\bar{1}4\}$ but the calcite crystals from 0.02 mol/dm^3 exhibited simple rhombohedral cleavages while the other calcites precipitated from 0.2 mol/dm^3 solution exhibited intergrowths of more numerous, smaller and thinner crystallites of $\{10\bar{1}4\}$ (Fig. 2). This behavior is often noticed from moderate to high supersaturated solutions in this study. The calcite precipitated from 0.4 mol/dm^3 $[Ca]_T$ solution also exhibited rhombohedral cleavage of $\{10\bar{1}4\}$, but it frequently showed a

modified morphology. The sharp rhombic {$10\bar{1}4$} faces were slightly modified along two of their edges as described by Paquette and Reeder (1995). The modified surface of this type exhibited more or less rounded surface.

Vaterite Crystals from the Solutions of $[CO_3]_T/[Ca]_T < 1$

The calcium carbonate crystals of the oolitic surface morphology were obtained when $[CO_3]_T/[Ca]_T < 1$ (Fig. 3). SEM and XRD analyses confirmed that the $CaCO_3$ crystals precipitated from these conditions were almost pure vaterite (Fig. 3 and 4). The morphology of vaterite precipitates, the hexagonal polymorphs of $CaCO_3$, also slightly changed depending on the degree of the supersaturation. With increasing $[Ca]_T$ from 0.02 mol/dm^3 to 0.4 mol/dm^3, the morphology of vaterite changed from a simple radial bundle to an aggregates having more complicated growth surfaces. Agglomeration of several unit of ellipsoidal sphere was more evident from the solutions of higher supersaturation such as 0.2 mol/dm^3 and 0.4 mol/dm^3 $[Ca]_T$ and it showed intergrowth of numerous and smaller crystallites (Fig. 3 and 4). As a result the surface areas of vaterite increased as the surface morphology became complicated with irregular ellipsoidal shape.

Surface Area in Relation to the Morphology and the Crystal Size

Table 2 presents the calculated saturation indices of each experimental solution with respect to calcite ($K_{sp} = 10^{-8.48}$). The saturation indices of 0.02 mol/dm^3, 0.2 mol/dm^3, and 0.4 mol/dm^3 $Ca]_T$ solutions ranges 11.78~12.38, 13.78~14.38, and 14.38~14.99, respectively (Table 2). Calculated saturation indeces were plotted against calcium concentration (Fig. 5). According to Fig. 5, it appears that the surface areas of $CaCO_3$ precipitates were mainly affected not by the calcium concentration but by the carbonate concentration during spontaneous precipitation. In general, the decreased carbonate concentration resulted in increasing surface roughness and increasing surface areas. For example, the surface roughness of vaterite increased with decreasing $[CO_3]_T$, $[CO_3]_T/[Ca]_T$ ratio from 0.8 to 0.5, and consequently the surface areas of vaterite increased from 5.64~7.34 to 8.39~10.3 (Table 2 and Fig. 5).

Table 2. Calculated saturation index of the $CaCO_3$ crystals precipitated by spontaneous nucleation.

$[Ca]_T$ (mol/dm^3)	$[CO_3]_T$ (mol/dm^3)	Saturation index (Ω)
0.02	0.01~0.04	11.78~12.38
0.2	0.1~0.4	13.78~14.38
0.4	0.2~0.8	14.38~14.99

The saturation index (Ω) of the calcium carbonate precipitating systems were calculated based on this:

$$\Omega = Q/K_{SP} \text{ where } Q = [H]/[Ca^{+}][HCO_3^{-}]$$

in which the brackets refer to activities of dissolved ion in solution, Q is the ion activity product, and K_{sp} is the solubility product of calcium carbonate

Two obvious variables reveal to the factors affect the surface area of $CaCO_3$ precipitate, crystal size and surface morphology represented by the surface roughness. As the grain size increased, the surface areas decreased. But the increased surface roughness will increase the surface area. Within the solutions where the total carbonate concentration was equal or greater than total calcium concentration, the calcite crystal of lower surface area was precipitated. On the other hand, the vaterite crystals of higher surface area were precipitated from the solution of lower total carbonate concentration than total calcium concentration. In Table 1, the surface areas of calcite show a maximum value of 1.56 m^2/g while the surface areas of vaterite are between 5.64 and 10.3 m^2/g. Although the mean size of both calcite and vaterite were similar, the fundamental differences in the nature of surfaces would lead to a significant difference in the available surface areas, which might provide different surface conditions on mineral-water interfacial reactions.

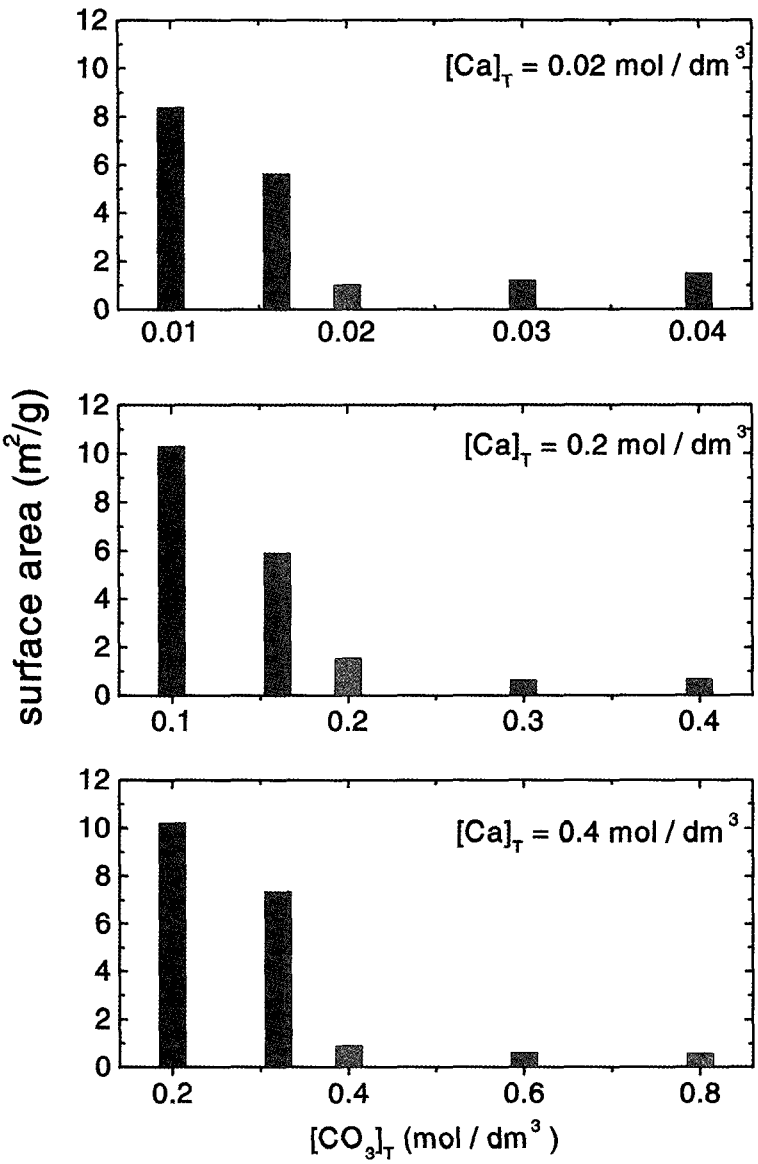

Fig. 5. The surface areas of synthetic $CaCO_3$ crystals are plotted against $[CO_3]_T$ (mol/dm^3).

Implications of Surface Morphology to Available Site for Sorption

Surface-sensitive microscopic and spectroscopic techniques demonstrated the occurrences and the densities of the surface complexes such as $\equiv CO_3H$ and $\equiv CaOH$, which plays an important role for metals interaction with $CaCO_3$ surfaces (Stipp and Hochellar, 1991; Cappellen *et al.*, 1993). The chemical structure and the reactivity of surface sites were considered as a strong factor affecting the reaction processes of forming different surface complexes during calcite-water interactions.

Titiloye *et al.* (1998) presented the difference of carbonate minerals surface structures with

characteristic surface energies. Each face on calcite and dolomite surfaces exhibits different surface energies depending on their crystallographic orientations. According to their atomistic simulation, the surface energies of stable $\{10\bar{1}4\}$ and $\{10\bar{1}0\}$ faces are lower than those of $\{11\bar{2}0\}$ face, 0.590, 0.970, and 1.390 J/m^2, respectively. The surface energy was assumed to determine the equilibrium surface morphology (Titiloye *et al.*, 1998; Leeuw and Parker, 1998). The equilibrium surface morphology was considered as a visual guide to the changes in surface stability during mineral-water interactions. The densities of surface sites with distinctive site energies would control the mineral-water interfacial reactions in terms of preferred removal of impurity ions or differential dissolution behaviors (Hillner *et al.*, 1992).

The carbonate mineral surfaces having more complicated surface morphologies such as small steps and kinks will have higher energy surface sites. The increased population density of high-energy surface sites drives more accumulation of common trace metals during mineral-water interactions.

Minerals formed in various natural systems provide a record of the physicochemical processes of their formation and the environmental factors that regulate their formation. In addition, geochemical record on the mineral surface reflects the environmental history of their formation. Surface morphology of various carbonate minerals may control the preferred sorption and subsequence surface precipitation behavior of common metal ion from the natural systems. In calcium carbonate precipitates, the surfaces with higher energy sites would prefer to sorb more trace metals, while the surfaces of more stable sites would prefer to sorb less trace metals. Along this, the kinetics of the surface reaction with metal ions would be another important factor to control the metal ion removal process by solid surface. Fast sorption kinetics is expected from the surfaces with much higher energy sites and relatively slower sorption kinetics is expected from the surfaces of more stable sites with lower energy. Therefore, a better insight into the mechanisms of the individual processes would be of great help in understanding metal ions interaction processes in natural environments.

Conclusions

Each $CaCO_3$ crystals exhibited characteristic surface morphologies depending on their solution compositions. XRD analysis and SEM observation reveal that the $CaCO_3$ precipitates prepared from the solutions of $[CO_3]_T / [Ca]_T \geq 1$ were mostly calcite precipitates, while $CaCO_3$ precipitates prepared from $[CO_3]_T / [Ca]_T < 1$ conditions were almost pure vaterite, a $CaCO_3$ polymorph of calcium carbonate. Although there was a small quantity of both vaterite and calcite impurities were present, the amount of those phases was very limited.

The $CaCO_3$ precipitated from the solutions of different supersaturation conditions demonstrated a direct relationship among the observed surface morphologies, the surface areas, and the size of each $CaCO_3$ precipitates. As the grain size increased, the surface areas decreased. And the increased surface roughness increased the surface areas. The measured surface area of calcite showed a maximum value of 1.56 m^2/g while the maximum surface area of vaterite was 10.3 m^2/g although the mean size of both calcite and vaterite were similar. The fundamental differences in the nature of surfaces would lead to form different surface morphologies as well as different reactivity for each metal interested. The increased surface areas as well as the increased number of high energy surface site may play an important control on the metal ion surface reactions during removal or dissolution processes.

References

Cappellen V. P., Charlet L., Stumm W., and Wersin P. (1993) A surface complexation model of the carbonate mineral-aqueous solution interface. Geochim. Cosmochim. Acta 57, 3505-3518.

Comans R.N. and J.J. Middelburg (1987) Sorption of trace metals on calcite:applicability of the surface precipitation model. Geochim. Cosmochim. Acta 51, 2587-2591.

Davis J.A., C.C. Fuller, and A.D. Cook (1987) A model for trace metal sorption processes at the calcite surface: adsorption of Cd^{2+} and subsequent solid solution formation. Geochim. Cosmochim. Acta 51, 1477-1490.

Dove P. M. and Hochella M. F. (1993) Calcite precipitation mechanisms and inhibition by orthorphosphate: In situ observation by Scanning Force Microscopy. Geochim. Cosmochim. Acta 57, 705-714.

Hillner P. E., Manne S., Gratz A. J., and Hansma P. K. (1992) AFM images of dissolution and growth on a calcite crystal. Ultamicroscopy 42-44, 1387-1393.

Kile D. E., Eberl D. D., Hoch A. R., and Reddy M. M. (2000) An assessment of calcite crystal growth mechanisms based on crystal size distributions. Geochim. Cosmochim. Acta 64, 2937-2950.

Leeuw N. H. and Parker S. C. (1998) Surface structure and morphology of calcium carbonate polymorphs calcite, aragonite, and vaterite: An atomistic approach. J. Phys. Chem., B 102, 2914-2922.

Liang Y. and Baer D. R. (1997) Anisotropic dissolution at the $CaCO_3$ (104)-water interface. Surface science 373, 275-287.

Miyazaki K. (1996) A numerical simulation of textural evolution due to Ostwald ripening in metamorphic rocks: A case for small amount of volume of dispersed crystals. Geochim. Cosmochim. Acta 60, 227-290.

Mullin J. W. (1991) Crystallization. Butterworth-Heinemann 291-308.

Paquette J. and Reeder R.J. (1995) Relationship between surface structure, growth mechanism, and trace element incorporation in calcite. Geochim. Cosmochim. Acta 59, 735-749.

Reeder R.J. (1996) Interaction of divalent cobalt, zinc, cadmium, and barium with the calcite surface during layer growth. Geochim. Cosmochim. Acta 60, 1543-1552.

Stipp S. L. and Hochellar M. F. Jr. (1991) Structure and bonding environments at the calcite surfaces as observed with x-ray photoelectron spectroscopy (XPS) and low-energy electron diffraction (LEED). Geochim. Cosmochim. Acta 55, 1723-1736.

Titiloye J. O., N.H. DE Leeuw, and Parker, S. C. (1998) Atomistic simulation of the differences between calcite and dolomite surfaces. Geochim. Cosmochim. Acta 62, No15, 2637-2641.

Zachara J.M., Cowan C.E., and C.T. Resch (1991) Sorption of divalent metals on calcite. Geochim. Cosmochim. Acta 55, 1549-1562.

2004년 2월 17일 원고접수, 2004년 3월 11일 게재승인.